the absence of ONO-1301 (Fig. 1A). To investigate the BMC migration toward ONO-1301-treated NHDF conditioned medium, a migration assay was performed using a modified Boyden chamber with 8-μm pores. The number of migrated BMCs was significantly greater in the conditioned medium of cells treated with 100 and 1000 nM ONO-1301 compared to that of cells treated with 0 and 10 nM ONO-1301. The BMC migration to the 1000 nM ONO-1301 conditioned medium was diminished by treating the BMCs with a CXCR4-neutralizing antibody or CXCR4 antagonist (AMD3100) (Fig. 1B, C).

SDF-1-mediated BMC Accumulation in the ONO-1301-treated Infarcted Hearts

The effect of ONO-1301 on SDF-1 expression in the infarcted hearts was evaluated by quantitative RT-PCR. Twenty-eight days after treatment, the SDF-1 expression in the border area of the ONO-1301-treated heart was significantly greater than that in the vehicle-treated heart (Fig. 2A). The HGF and VEGF expressions were also increased by ONO-1301 treatment (Fig. 2B, C). After LAD occlusion, ONO-1301 treatment, and intravenous injection of labeled BMCs, the BMC accumulation in the infarcted heart was evaluated by an in vivo imaging system. The proportion of BMCs in the heart showed a trend toward upregulation, dependent on the dose of ONO-1301 (Fig. 2D). Hearts treated with 100 mg ONO-1301/kg body weight showed significantly more accumulated BMCs than those treated with 0 or 10 mg ONO-1301. In 100 mg/kg ONO-1301-treated hearts, CXCR4 antagonization significantly decreased the BMC accumulation (Fig. 2D). To identify the recruited BMCs *in vivo*, the acute MI model was prepared using chimera mice by transplanting GFP-expressing bone marrow into irradiated C57BL/6 mice. The BMCs of the C57BL/6 transplant recipients were largely replaced by GFP-expressing BMCs (91.8+/−4.3%, figure S1 in File S1). The single-organ analyses using GFP-BM chimera mouse at day 7 also showed increased BMC accumulation in the ONO-1301-treated myocardium (figure S2 in File S1).

Differentiation of BMCs in the Infarcted Myocardium

Seven days after MI and ONO-1301 administration to BM-GFP chimera mouse, BMCs were dramatically accumulated in both the infarcted area and the atelocollagen sheet (Fig. 3A, B). Some of the BMCs formed tube-like structures and displayed von Willebrand factor expression (Fig. 3C, D). Isolectin staining showed that a greater percentage of isolectin-positive BMCs accumulated in the myocardium in the ONO-1301-treated (O) group than in the vehicle (V) group (Fig. 3E, F). We also evaluated small blood vessels by CD31 immunostaining. The density of small vessels was greater in the O group than in the V group (Fig. 3G). Immunohistochemical analysis of Connexin 43 and smooth muscle actin, cardiac-lineage and cardiac fibroblast markers, respectively, was also conducted at 3 months, but no co-expression

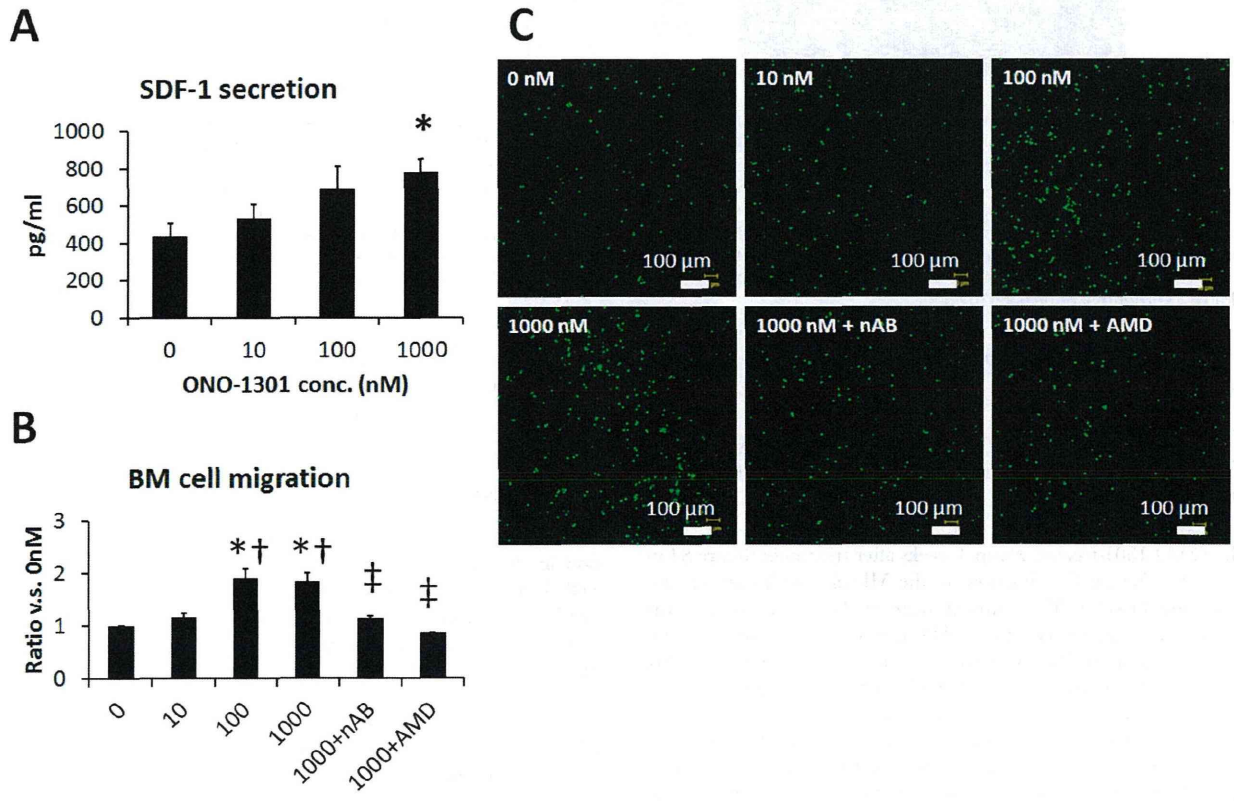

Figure 1. ONO-1301 enhanced SDF-1 secretion and BMC migration via SDF-1/CXCR4 signaling *in vitro*. NHDFs were stimulated with ONO-1301 for 72 hours, then the SDF-1 concentration in the culture medium was determined by ELISA (n = 3 each, *P<0.05 vs. 0 nM). A) Number of BMCs that migrated toward the conditioned medium from ONO-1301-stimulated-NHDFs (0, 10, 100, or 1000 nM ONO-1301, n = 6; 1000 nM+nAB or 1000 nM+AMD, n = 3). *P<0.05 vs. 0 nM, †P<0.05 vs. 10 nM, ‡P<0.05 vs. 1000 nM, §P<0.05 vs. SDF-1. nAB, CXCR4-neutralizing antibody; AMD, CXCR4 antagonist AMD3100. B) Representative pictures of BMCs that had migrated to the medium from ONO-1301-stimulated BMCs. Green, BMCs.
doi:10.1371/journal.pone.0069302.g001

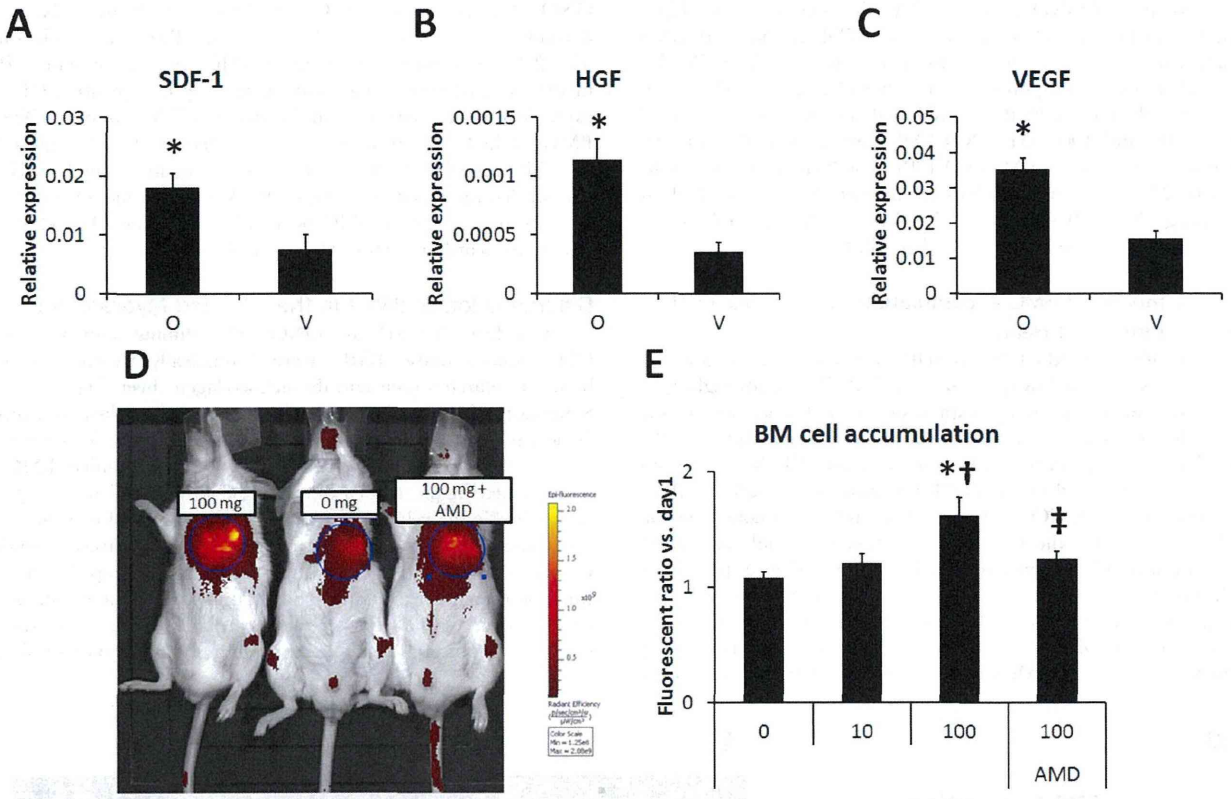

Figure 2. ONO-1301 enhanced SDF-1 secretion and BMC migration via SDF-1/CXCR4 signaling after MI. A–C) The SDF-1, HGF, and VEGF expression at the border zone of the infarcted area was measured by quantitative RT-PCR. The expression levels of these cytokines were higher in the ONO-1301-treated (O) group compared to the vehicle (V) group. (O group, n = 7; V group, n = 7–8; *$P<0.05$ vs. V group). The expression relative to GAPDH is shown. D) BMC migration to ONO-1301-treated infarcted myocardium was evaluated using IVIS. Representative picture of IVIS at day 3. Left: 100 mg/Kg, Center: 0 mg/Kg, Right: 100 mg/Kg+AMD3100 (AMD). E) The number of accumulated BMCs was greater in the 100 mg/kg ONO-1301-treated infarcted heart compared to the 0 and 10 mg/kg ONO-1301-treated infarcted heart. When BMCs treated with AMD were injected, the BMC accumulation decreased in the 100 mg/Kg ONO-1301-treated infarcted heart compared with the untreated-BMC-injected heart (0 mg/Kg, n = 4; 10 mg/Kg, n = 8; 100 mg/Kg, n = 5; 100 mg/Kg+AMD3100, n = 4; *$P<0.05$ vs. 0 mg/Kg, †$P<0.05$ vs. 10 mg/Kg, ‡$P<0.05$ vs. 100 mg/Kg).
doi:10.1371/journal.pone.0069302.g002

of GFP with either of these markers was observed (figure S3 in File S1).

Therapeutic Effects of ONO-1301 Administration on Cardiac Performance, Survival, and LV-remodeling at 4 Weeks Post-MI

ONO-1301 was detected in the plasma of blood samples from the ONO-1301-treated group 3 weeks after treatment (figure S4 in File S1). The cardiac functions in the MI mice with and without following ONO-1301 treatment were evaluated. Mortality was substantial until 14 days post-LAD ligation in the vehicle group, and similar mortality levels were observed with non-treated MI mice [11]. In contrast, in the ONO-1301-treated group, there was little mortality 7 days after MI, and thus a difference in survival (Fig. 4A). Cardiac performance was evaluated by 2D echocardiography 4 weeks after implantation. The LVEDA was smaller in the ONO-1301-treated group than in the vehicle group, but the difference was not significant. In contrast, the LVESA was significantly smaller, and the LVFAC was significantly greater, in the ONO-1301-treated group than in the vehicle group (Fig. 4B). In the histological analysis, the vehicle group showed a typical MI with a large anterior LV scar and dilatation of the LV cavity. By comparison, the LV of the ONO-1301-treated group was less dilated, and the anterior wall was thicker (Fig. 4C, D). The infarcted area and percent fibrosis were significantly smaller in the ONO-1301-treated than in the vehicle-treated group (Fig. 4C, E–G).

Discussion

Here, we showed that ONO-1301 promotes BMC accumulation in the injured myocardium. *In vitro*, ONO-1301 enhanced SDF-1 expression, and BMC migration was greater to conditioned medium obtained from ONO-1301-stimulated cells. The enhanced migration was diminished by blocking SDF-1/CXCR4 signaling. Consistent with the *in vitro* experiments, ONO-1301 enhanced the SDF-1 expression of myocardial tissue. High ONO-1301 accelerated the BMC accumulation after MI in a SDF-1/CXCR4-dependent manner. Some BMCs in the infarcted myocardium differentiated into capillary structures within 7 days. Furthermore, the sustained-release delivery of ONO-1301 in the infarcted myocardium also led to functional improvements following MI. Our data suggest that ONO-1301 is a novel inducer of BMC recruitment, and that ONO-1301 treatment may be a promising therapeutic strategy for the clinical treatment of MI.

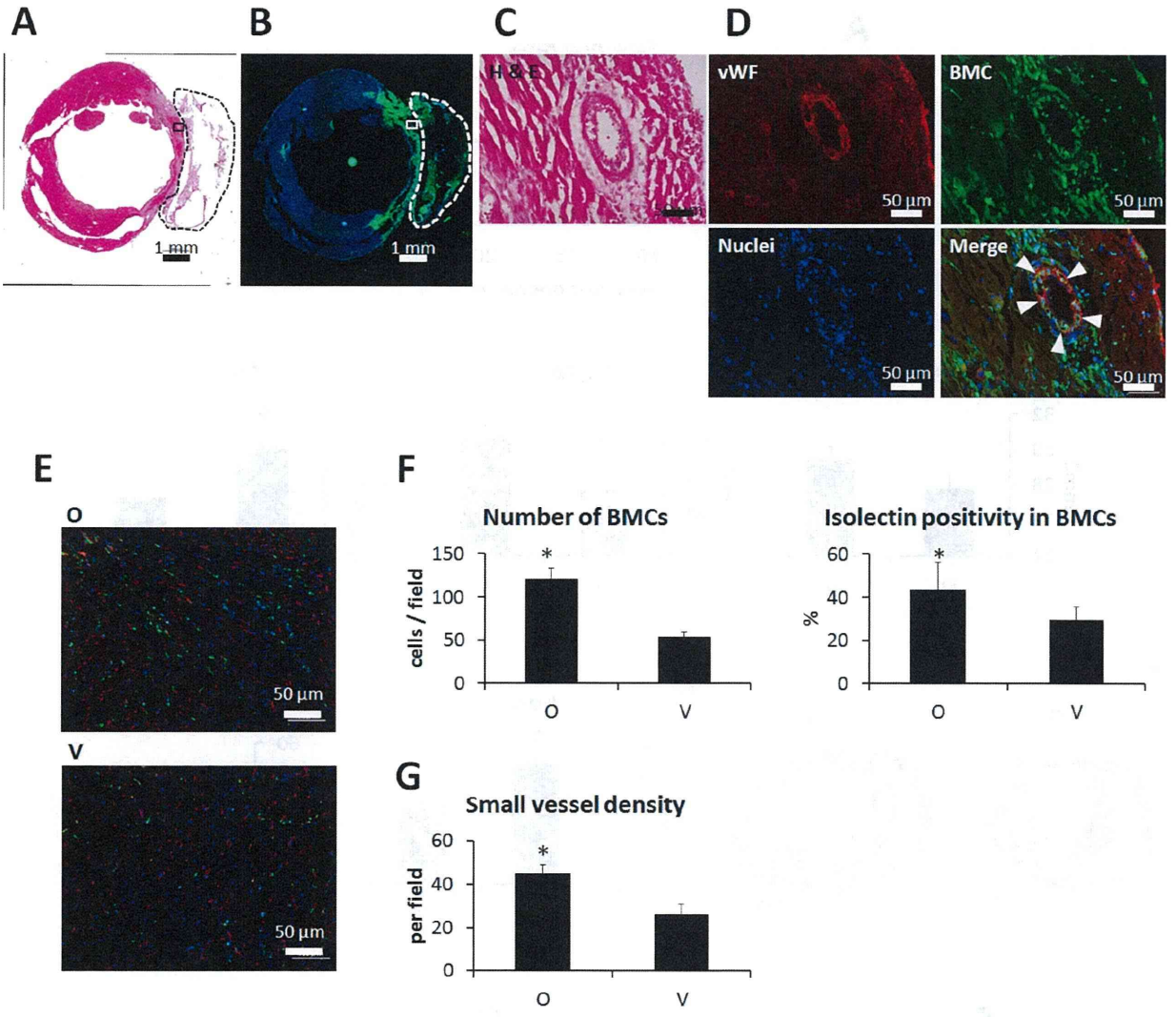

Figure 3. BMCs differentiated into capillary structures in the infarcted area after MI and ONO-1301 treatment. Representative macro image of H and E staining seven days after MI and ONO-1301 treatment. The transplanted sheet is enclosed by a dashed line. A) Serial section of A. The BMCs displayed GFP. B) High-magnification image of the boxed region in A. C) Serial section of C. Arrowheads indicate vWF-expressing BMCs. Red indicates vWF; green, BMCs; and blue, nuclei. D) Representative images of isolectin-stained BMCs seven days after MI and ONO-1301 treatment. E) BMC accumulation and percentages of isolectin-positive BMCs. The number of BMCs that accumulated in the infarcted myocardium was greater in the ONO-1301-treated (O) group than in the vehicle (V) group. The percentage of isolectin-positive BMCs was also greater in the O group than in the V group. *$P<0.05$ vs. V group. F) Small vessel density. Small vessels were detected by CD31 immunostaining. The density of small vessels in the O group was greater than in the V group. *$P<0.05$ vs. V group.
doi:10.1371/journal.pone.0069302.g003

It is difficult to understand the whole mechanism underlying the functional improvements induced by ONO-1301. It was already reported that ONO-1301 enhances the expression of angiogenic factors HGF and VEGF, leading to angiogenesis and the suppression of fibrosis progression [7,8,9]. In this study, we discovered an alternative mechanism for ONO-1301's therapeutic efficacy in the acute MI mouse, in which the upregulation of SDF-1 promotes BMC accumulation. Stem-cell recruitment and homing are regulated by the interplay of cytokines, chemokines, and proteases. In particular, the SDF-1/CXCR4 axis is central for the mobilization of stem cells from the bone marrow and their homing to ischemic tissues [12]. In the case of ischemic insult, SDF-1 is released by the injured tissue and stimulates the mobilization of progenitor cells from the bone marrow [1,13]. Furthermore, prostaglandins have been reported to facilitate BMC mobilization via upregulation of CXCR4 expression [14,15]. In our experimental setting, ONO-1301 was detected from peripheral blood samples 3 weeks after treatment (Fig. S4 in File S1), suggesting that ONO-1301 may similarly act on the bone marrow to promote the BMC mobilization. Thus, BMC recruitment in the injured myocardium may be enhanced by the upregulation of SDF-1 in cardiac fibroblasts and by the direct upregulation of CXCR4 in BMCs located in the bone marrow. In addition, recent reports show the possibility of endogenous regeneration in the injured heart, including proliferation of postnatal cardiomyocytes and cardiac stem cells [16,17,18,19]. While we were unable to

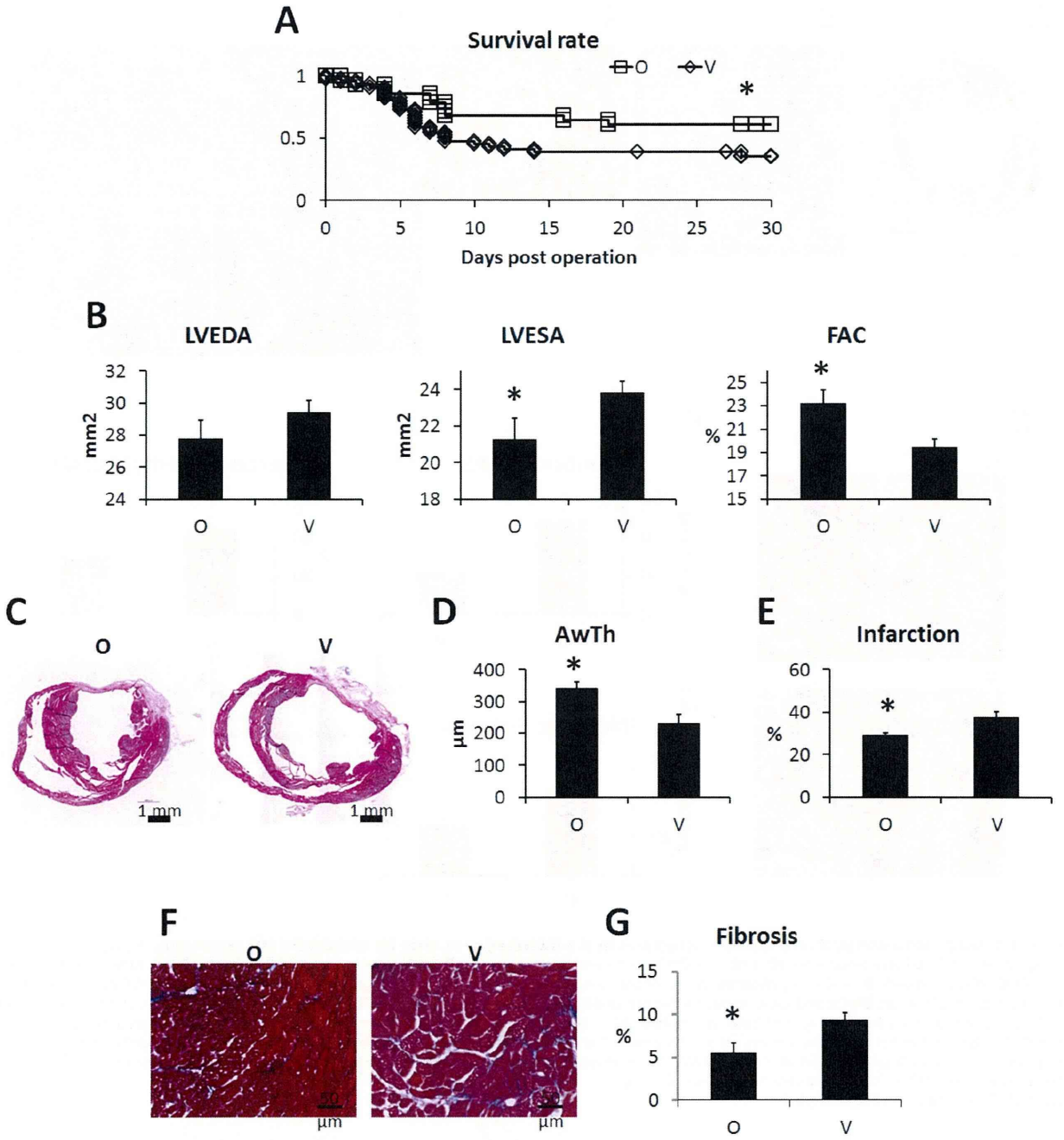

Figure 4. ONO-1301 treatment improved the cardiac performance and survival rate after MI. Survival rates after treatment. The ONO-1301-treated (O) group (n = 33) showed significantly better survival than the vehicle (V) group (n = 48). *P<0.05 vs. V group. A) Evaluation of cardiac performance 4 weeks after treatment. In the O group, the LVESA was smaller, and the FAC was significantly higher compared to the V group (O group, n = 22; V group, n = 20; *P<0.05 vs. V group). B) Representative macro images from each group. C) Quantification of anterior wall thickness. Anterior wall thickness was significantly thicker in the O group (n = 6) compared to the V group (n = 4). *P<0.05 vs. V group. D) Quantification of percent infarction. Infarction was significantly smaller in the O group (n = 6) compared to the V group (n = 4). *P<0.05 vs. V group. E) Representative Masson trichrome staining images at the border zone. F) Quantification of fibrosis. Fibrosis at the border zone was significantly smaller in the O group (n = 6) compared to the V group (n = 4). *P<0.05 vs. V group.
doi:10.1371/journal.pone.0069302.g004

detect newly-generated cardiomyocytes derived from BMCs in this study, it would be interesting to evaluate the possibility of cardiomyogenesis involving other cell types.

We observed massive BMC accumulation 7 days after MI, including in the infarcted ventricular wall, where they provided structural support in place of the necrotic cardiomyocytes. The

BMCs recruited into the infarcted myocardium may contain various kinds of somatic stem cells, such as endothelial progenitor cells [20], bone marrow-derived stem cells [21], and bone marrow mononuclear cells [2], which have potent therapeutic effects in heart failure [22]. Furthermore, bone marrow-derived mesenchymal stem cells secrete prostaglandin [23], which may act like ONO-1301 and amplify the effects of the ONO-1301-mediated therapy. Kawabe et al. clearly showed that prostaglandin facilitates the recruitment of endothelial progenitor cells [24]. Although further analysis is needed, the enhanced accumulation of BMCs may predispose the damaged heart tissue to better restoration following MI.

Many reports have shown that granulocyte colony-stimulating factor (G-CSF) and granulocyte-macrophage colony-stimulating factor (GM-CSF) also induce BMC mobilization, with therapeutic effects in animal models [25]. However, G-CSF therapy in unselected patients with acute MI did not lead to functional improvements beyond those achieved with conventional therapy. In addition, the administration of GM-CSF in cancer patients has been shown to transiently increase the LV end-systolic dimensions and decrease cardiac contractility [25,26]. The lack of efficacy of G-CSF therapy in clinical trials may be due, at least in part, to its poor initiation and duration; such therapies are likely to be most beneficial during the early phase after acute MI. Although conventional prostacyclin and its analogs are chemically and biologically unstable, ONO-1301 is a long-acting prostacyclin agonist that exerts stable effects *in vivo*, because it lacks a prostanoid structure. Furthermore, we used a slow-release form of ONO-1301, made by polymerizing it with poly-lactic and glycolic acid; this ONO-1301 could still be detected in the blood 3 weeks after its administration (figure S4 in File S1).

Furthermore, in our *in vitro* analysis, although we used normal human dermal fibroblasts to examine the SDF-1/CXCR-4-dependent BMC migration, the reactivity to ONO-1301 stimulation will differ depending on the cell type. For example, the G-CSF expression was upregulated in some kinds of cells (unpublished data). Thus, together with the upregulation of multiple beneficial cytokines such as HGF and VEGF, because of the longer duration of its activity, ONO-1301 may be more potent than conventional protein-based therapies.

Our data showed that ONO-1301 treatment was a potent inducer of BMC homing. Of the BMCs that accumulated in the infarcted myocardium, 43 percent expressed isolectin, an endothelial cell marker, but the other BMCs had a fibroblastic morphology, and did not express cardiac-lineage or cardiofibroblast markers (Figure S3 in File S1). ONO-1301 administration resulted in the attenuation of cardiac dysfunction, with enhanced BMC accumulation. Further study is required to elucidate the mechanism, but we speculate that paracrine effects of factors released by the BMCs play pivotal roles in the therapeutic efficacy, rather than the transdifferentiation of the BMCs into the cardiac or vascular lineage. The effect of cardioprotective and angiogenic factors secreted by the accumulated BMCs and the direct stimulation of ONO-1301 itself may synergistically increase the angiogenesis and cardioprotection, leading to improved therapeutic results.

In summary, ONO-1301 may be a powerful, long-acting activator of multiple cytokines. In particular, SDF-1 may enhance the BMC accumulation in a SDF-1/CXCR4-signaling-dependent manner, leading to an attenuation of the cardiac dysfunction following MI. Our findings suggest that the method involving a sustained release of ONO-1301 may be adapted as a novel drug delivery system for treating heart failure.

Supporting Information

File S1.
(DOCX)

Acknowledgments

We thank Masako Yokoyama and Akima Harada for their excellent technical assistance.

Author Contributions

Conceived and designed the experiments: YI SM Y. Sawa. Performed the experiments: YI KI NS. Analyzed the data: YI AS. Contributed reagents/materials/analysis tools: Y. Sakai. Wrote the paper: YI SM SF Y. Sawa.

References

1. Abbott JD (2004) Stromal cell-derived factor-1 plays a critical role in stem cell recruitment to the heart after myocardial infarction but is not sufficient to induce homing in the absence of injury. Circulation 110: 3300–3305.
2. Askari AT, Unzek S, Popovic ZB, Goldman CK, Forudi F, et al. (2003) Effect of stromal-cell-derived factor 1 on stem-cell homing and tissue regeneration in ischaemic cardiomyopathy. Lancet 362: 697–703.
3. Peled A (1999) Dependence of human stem cell engraftment and repopulation of NOD/SCID mice on CXCR4. Science 283: 845–848.
4. Yamaguchi Ji (2003) Stromal cell-derived factor-1 effects on ex vivo expanded endothelial progenitor cell recruitment for ischemic neovascularization. Circulation 107: 1322–1328.
5. Yamanaka S, Miura K, Yukimura T, Okumura M, Yamamoto K (1992) Putative mechanism of hypotensive action of platelet-activating factor in dogs. Circ Res 70: 893–901.
6. Sata M, Nakamura K, Iwata H, Sakai Y, Hirata Y, et al. (2007) A synthetic small molecule, ONO-1301, enhances endogenous growth factor expression and augments angiogenesis in the ischaemic heart. Clin Sci 112: 607.
7. Hirata Y, Soeki T, Akaike M, Sakai Y, Igarashi T, et al. (2009) Synthetic prostacycline agonist, ONO-1301, ameliorates left ventricular dysfunction and cardiac fibrosis in cardiomyopathic hamsters. Biomed Pharmacother 63: 781–786.
8. Yamasaki H, Maeshima Y, Nasu T, Saito D, Tanabe K, et al. (2011) Intermittent administration of a sustained-release prostacyclin analog ONO-1301 ameliorates renal alterations in a rat type 1 diabetes model. Prostaglandins Leukot Essent Fatty Acids 84: 99–107.
9. Nakamura K, Sata M, Iwata H, Sakai Y, Hirata Y, et al. (2007) A synthetic small molecule, ONO-1301, enhances endogenous growth factor expression and augments angiogenesis in the ischaemic heart. Clin Sci 112: 607–616.
10. Imanishi Y, Saito A, Komoda H, Kitagawa-Sakakida S, Miyagawa S, et al. (2008) Allogenic mesenchymal stem cell transplantation has a therapeutic effect in acute myocardial infarction in rats. J Mol Cell Cardiol 44: 662–671.
11. Imanishi Y, Miyagawa S, Maeda N, Fukushima S, Kitagawa-Sakakida S, et al. (2011) Induced adipocyte cell-sheet ameliorates cardiac dysfunction in a mouse myocardial infarction model: a novel drug delivery system for heart failure. Circulation 124: S10–17.
12. Ceradini DJ, Kulkarni AR, Callaghan MJ, Tepper OM, Bastidas N, et al. (2004) Progenitor cell trafficking is regulated by hypoxic gradients through HIF-1 induction of SDF-1. Nat Med 10: 858–864.
13. Zaruba MM, Franz WM (2010) Role of the SDF-1-CXCR4 axis in stem cell-based therapies for ischemic cardiomyopathy. Expert Opin Biol Ther 10: 321–335.
14. Goichberg P (2005) cAMP-induced PKCzeta activation increases functional CXCR4 expression on human CD34+ hematopoietic progenitors. Blood 107: 870–879.
15. North TE, Goessling W, Walkley CR, Lengerke C, Kopani KR, et al. (2007) Prostaglandin E2 regulates vertebrate haematopoietic stem cell homeostasis. Nature 447: 1007–1011.
16. Leri A, Kajstura J, Anversa P (2011) Role of cardiac stem cells in cardiac pathophysiology: a paradigm shift in human myocardial biology. Circ Res 109: 941–961.
17. Smith RR, Barile L, Cho HC, Leppo MK, Hare JM, et al. (2007) Regenerative potential of cardiosphere-derived cells expanded from percutaneous endomyocardial biopsy specimens. Circulation 115: 896–908.
18. Mollova M, Bersell K, Walsh S, Savla J, Das LT, et al. (2013) Cardiomyocyte proliferation contributes to heart growth in young humans. Proc Nat Acad Sci U S A 110: 1446–1451.

19. Kajstura J, Rota M, Cappetta D, Ogorek B, Arranto C, et al. (2012) Cardiomyogenesis in the aging and failing human heart. Circulation 126: 1869–1881.
20. Asahara T, Murohara T, Sullivan A, Silver M, van der Zee R, et al. (1997) Isolation of putative progenitor endothelial cells for angiogenesis. Science 275: 964–967.
21. Orlic D, Kajstura J, Chimenti S, Limana F, Jakoniuk I, et al. (2001) Mobilized bone marrow cells repair the infarcted heart, improving function and survival. Proc Natl Acad Sci U S A 98: 10344–10349.
22. Smart N, Riley PR (2008) The stem cell movement. Circ Res 102: 1155–1168.
23. Matysiak M, Orlowski W, Fortak-Michalska M, Jurewicz A, Selmaj K (2011) Immunoregulatory function of bone marrow mesenchymal stem cells in EAE depends on their differentiation state and secretion of PGE2. J Neuroimmunol 233: 106–111.
24. Kawabe J, Yuhki K, Okada M, Kanno T, Yamauchi A, et al. (2010) Prostaglandin I2 promotes recruitment of endothelial progenitor cells and limits vascular remodeling. Arterioscler Thromb Vasc Biol 30: 464–470.
25. Sanganalmath SK, Abdel-Latif A, Bolli R, Xuan YT, Dawn B (2011) Hematopoietic cytokines for cardiac repair: mobilization of bone marrow cells and beyond. Basic Res Cardiol 106: 709–733.
26. Knoops S, Groeneveld ABJ, Kamp O, Lagrand WK, Hoekman K (2001) Granulocyte-macrophage colony-stimulating factor (GM-CSF) decreases left ventricular function. an echocardiographic study in cancer patients. Cytokine 14: 184–187.

A slow-releasing form of prostacyclin agonist (ONO1301SR) enhances endogenous secretion of multiple cardiotherapeutic cytokines and improves cardiac function in a rapid-pacing–induced model of canine heart failure

Tomonori Shirasaka, MD,[a] Shigeru Miyagawa, MD, PhD,[b] Satsuki Fukushima, MD, PhD,[b] Atsuhiro Saito, PhD,[b] Motoko Shiozaki, PhD,[b] Naomasa Kawaguchi, PhD,[c] Nariaki Matsuura, MD, PhD,[c] Satoshi Nakatani, MD, PhD,[d] Yoshiki Sakai, PhD,[e] Takashi Daimon, PhD,[f] Yutaka Okita, MD, PhD,[a] and Yoshiki Sawa, MD, PhD[b]

Objectives: Cardiac functional deterioration in dilated cardiomyopathy (DCM) is known to be reversed by intramyocardial up-regulation of multiple cardioprotective factors, whereas a prostacyclin analog, ONO1301, has been shown to paracrinally activate interstitial cells to release a variety of protective factors. We here hypothesized that intramyocardial delivery of a slow-releasing form of ONO1301 (ONO1301SR) might activate regional myocardium to up-regulate cardiotherapeutic factors, leading to regional and global functional recovery in DCM.

Methods and Results: ONO1301 elevated messenger RNA and protein level of hepatocyte growth factor, vascular endothelial growth factor, and stromal-derived factor-1 of normal human dermal fibroblasts in a dose-dependent manner in vitro. Intramyocardial delivery of ONO1301SR, which is ONO1301 mixed with polylactic and glycolic acid polymer (PLGA), but not that of PLGA only, yielded significant global functional recovery in a canine rapid pacing–induced DCM model, assessed by echocardiography and cardiac catheterization (n = 5 each). Importantly, speckle-tracking echocardiography unveiled significant regional functional recovery in the ONO1301-delivered territory, consistent to significantly increased vascular density, reduced interstitial collagen accumulation, attenuated myocyte hypertrophy, and reversed mitochondrial structure in the corresponding area.

Conclusions: Intramyocardial delivery of ONO1301SR, which is a PLGA-coated slow-releasing form of ONO1301, up-regulated multiple cardiotherapeutic factors in the injected territory, leading to region-specific reverse left ventricular remodeling and consequently a global functional recovery in a rapid-pacing–induced canine DCM model, warranting a further preclinical study to optimize this novel drug-delivery system to treat DCM. (J Thorac Cardiovasc Surg 2013;146:413-21)

Dilated cardiomyopathy (DCM) is characterized by progressive and severe deterioration of cardiac function, eventually leading to advanced heart failure necessitating surgical interventions such as cardiac transplantation[1] or mechanical assist device implantation,[2] despite maximum currently available medical therapy including angiotensin-converting enzyme inhibitor[3] or beta-blocker.[4] Despite a variety of etiologies in DCM, the diseases consistently include pathologic hypertrophy of cardiomyocytes associated with mitochondrial dysfunction, increased interstitial fibrosis, and limited regional blood flow.[5-7] Pathologic left ventricular (LV) remodeling is reportedly reversed, at least in part, by cell transplantation that intramyocardially up-regulates multiple cardiotherapeutic cytokines in a constitutive manner.[8,9] However, cell therapy is limited in the clinical arena owing to availability of cell processing center or ethical issues. Therefore, synthetic reagents that yield similar cardiotherapeutic effects to cell transplantation have been sought.

Prostacyclin is an endogenous factor released by endothelial cells, activating endothelial cells, fibroblasts, or smooth muscle cells in an autocrine and paracrine manner to release multiple growth factors or cytokines, consequently producing local and systemic anti-inflammatory, antifibrotic, proangiogenic, and antithrombotic effects. However, clinical use of synthetic prostacyclin or prostacyclin analogs, such as epoprostenol and beraprost, for chronic diseases is hampered by its chemical instability[10,11] and therefore the delivery method.

ONO1301 is a synthetic prostacyclin analog having a unique structural feature to maintain chemical stability,

From the Division of Cardiovascular Surgery,[a] Kobe University Graduate School of Medicine, Kobe; the Division of Cardiovascular Surgery,[b] Osaka University Graduate School of Medicine, Suita; the Department of Molecular Pathology,[c] Graduate School of Medicine and Health Sciences, Division of Functional Diagnostics,[d] Department of Health Sciences, Osaka University Graduate School of Medicine, Osaka; Ono Pharmaceutical Company Ltd,[e] Osaka; and the Division of Biostatistics,[f] Hyogo College of Medicine, Hyogo, Japan.

Disclosures: Yoshiki Sakai is an employee of ONO pharmaceutical Co Ltd. All other authors have nothing to disclose with regard to commercial support.

Received for publication July 27, 2012; revisions received Sept 8, 2012; accepted for publication Oct 2, 2012; available ahead of print April 1, 2013.

Address for reprints: Yoshiki Sawa, MD, PhD, Osaka University Graduate School of Medicine, Suita, Japan, E1: 2-2 Yamadaoka, Suita, Osaka 565-0871, Japan (E-mail: sawa@surg1.med.osaka-u.ac.jp).

0022-5223/$36.00

http://dx.doi.org/10.1016/j.jtcvs.2012.10.003

Abbreviations and Acronyms

DCM	= dilated cardiomyopathy
Dd	= end-diastolic left ventricular dimension
Ds	= end-systolic left ventricular dimension
E	= early transmitral filling wave
E′	= early diastolic velocity of the mitral annulus
EF	= ejection fraction
EDWT	= end-diastolic wall thickness
ELISA	= enzyme-linked immunosorbent assay
ESWT	= end-systolic wall thickness
HGF	= hepatocyte growth factor
LV	= left ventricular (ventricle)
mRNA	= messenger RNA
ONO1301SR	= slow releasing form of ONO1301
PCR	= polymerase chain reaction
PLGA	= polylactic and glycolic acid polymer
SDF-1	= stromal-derived factor-1
VEGF	= vascular endothelial growth factor

possibly allowing slow-releasing system.[12] Of note, ONO1301 reportedly activates fibroblasts to release multiple factors such as hepatocyte growth factor (HGF) and vascular endothelial growth factor (VEGF),[13] both of which are known to be cardiotherapeutic.[14,15] Nakamura and associates[13] reported that direct intramyocardial injection of ONO1301 yielded cardiotherapeutic effects in a model of acute myocardial infarction in the mouse. On the other hand, Hirata and colleagues[16] reported that subcutaneous injection of ONO1301 improves global cardiac function associated with globally reduced fibrosis and increased capillaries in a hamster DCM model. However, it remains unclear that intramyocardial delivery of ONO1301 would produce therapeutic effects on a model of DCM heart failure in a large animal.

We therefore hypothesized that intramyocardial injection of ONO1301 might activate regional interstitial cells including fibroblasts in the injected area to locally upregulate multiple therapeutic factors, leading to region-specific functional recovery in DCM. Thus, we investigated therapeutic effects of local administration of a slow-releasing form of ONO1301 on regional cardiac function of DCM heart by using the canine rapid-pacing induction that is an established DCM model.[17,18]

METHODS

Animal Care

All studies were performed with the approval of the institutional ethics committee in Osaka University Graduate School of Medicine. All animals were treated in compliance with the "Principles of Laboratory Animal Care" (the National Society for Medical Research) and the "Guide for the Care and Use of Laboratory Animals" (National Institutes of Health publication). Human dermal fibroblasts were treated in compliance with the principles outlined in the Declaration of Helsinki. All procedures and analysis were carried out in a blinded manner. We had full access to and take full responsibility for the integrity of data and agree to the manuscript as written.

Culture of Human Dermal Fibroblasts With ONO1301 Added

Human dermal fibroblast cell line (NHDF; CryoNHDF Neo, Lonza, Switzerland) was cultured in fine bubble mixing culture (FGM-2 Bulletkit, Lonza) containing 2% fetal bovine serum. ONO1301 (0.1-1.0 μmol/mL) was added for 72 hours after serum-free culture for 24 hours.

Generation of a Slow-Releasing Form of ONO1301

A slow releasing form of ONO1301 (ONO1301SR; Ono Pharmaceutical Co Ltd, Osaka, Japan) was created by polymerization of ONO1301 with polylactic and glycolic acid polymer (PLGA) as described previously.[19] In brief, ONO1301 (5 mg) was mixed with 100 mg of PLGA in 0.1% polyvinyl alcohol with an equal molar ratio of lactic acid/glycolic acid. Releasing time of ONO1301SR in vitro was between about 14 days to 25 days, as determined by measuring residual ONO1301 in the pellets by liquid chromatography.

Generation of Canine DCM Model and Intramyocardial ONO1301SR Injection

Beagles weighing 10 kg (Oriental Yeast Co Ltd, Tokyo, Japan) were endotracheally intubated and supported by mechanical ventilation under general anesthesia using intravenous sodium pentobarbitual (6 mg/kg) for induction and inhaled sevoflurane (1%-2%) for subsequent maintenance. We maintained the adequacy of anesthesia evaluated by giving the dogs electrical stimuli every 30 minutes. This evaluation was performed during each operation for each procedure. The heart was exposed via the left fifth intercostal space, and 2 bipolar pacing leads (FINELINE II EZ STEROX; Boston Scientific, Boston, Mass) were attached on the free wall of the right ventricle, connected to a pulse generator (INSIGNIA I, Boston Scientific) placed in subcutaneous pocket. The ventricle was continuously paced at 240 beats/min for 8 weeks.[18]

Four weeks after rapid pacing commenced, either ONO1301SR or PLGA polymer only was injected with a 26-gauge needle at 5 points of lateral wall of the LV at regular intervals (total 15 mg of ONO1301 or PLGA polymer was injected, ONO1301SR group and control group, n = 5 each). Rapid pacing was temporally discontinued during the injection procedure, and it was set back at 240 beats/min the day after each operation. Dogs kept on rapid pacing for 8 weeks were humanely killed under general anesthesia with an overdose of intravenous sodium pentobarbitual (18 mg/kg) to achieve complete sedation followed by administration of potassium-based solution intravenously to assure that they were completely dead. The hearts were retrieved at 4 weeks after injection of either ONO1301SR or PLGA only. We here defined lateral LV wall where ONO1301SR was directly injected as the "target site" and the septal wall as the "remote site."

Conventional and Speckle-Tracking Echocardiography and Cardiac Catheterization

Transthoracic echocardiography (Altida; Toshiba Medical Systems Corporation, Tochigi, Japan) was performed under general anesthesia by 1% sevoflurane inhalation. End-diastolic and end-systolic LV dimensions (Dd and Ds, respectively) and end-systolic and end-diastolic wall thickness (ESWT and EDWT, respectively) of the target site and remote site were measured at mid-LV short axis view by conventional echocardiography. LV ejection fraction (EF) was calculated with biplanar Simpson's rule

from the apical 4-chamber view. E/E′, an indicator of diastolic function, was calculated by measuring peak Doppler velocities of early transmitral filling wave (E) and the peak early diastolic velocity of the mitral annulus (E′).

Speckle-tracking echocardiography and an offline software (Altida Extend; Toshiba Medical Systems Corporation) were used to measure radial, circumferential, transverse, and longitudinal strains to quantitatively assess regional LV wall motion.[20] Radial and circumferential strains were measured from the mid-LV short-axis view, whereas transverse and longitudinal strains were from the apical 4-chamber view.

Cardiac catheterization was performed under general anesthesia using 1% sevoflurane inhalation. A 3F micromanometer-tipped catheter (SPR-249; Millar Instruments, Inc, Houston, Tex) was inserted through the LV apex to measure heart rate, LV maximal systolic pressure, maximal rate of the LV pressure change evaluating systolic preload-dependent LV function, and time constant of LV relaxation (τ) evaluating diastolic load-dependent function.

Real-Time Polymerase Chain Reaction

Total RNA was retrieved from NHDF by using RNeasy Mini kit (Qiagen, Venlo, The Netherlands) and treated with RNase-Free DNase Set (Qiagen). TaqMan probes were designed using Primer Express software (Applied Biosystems, Carlsbad, Calif). Real-time polymerase chain reaction (PCR) was performed using a 7500 Fast Real-Time PCR System with TaqMan Universal PCR Master Mix (Applied Biosystems). Concentration of HGF, VEGF, and stromal-derived factor-1 (SDF-1) in the culture supernatant of NHDF was measured by using an enzyme-linked immunosorbent assay (ELISA) kit (Procarta Cytokine Assay kit, Panomics, Santa Clara, Calif).

Histologic Analysis and Electron Microscopy

The extracted dog hearts were transversely cut, fixed with 10% buffered formalin, and embedded in paraffin. The heart sections of 10-μm thickness were stained with hematoxylin and eosin, Masson-trichrome, picro-sirius red, and periodic acid–Schiff. The heart sections were also labeled by anti-von Willebrand factor antibody (Dako EPOS) visualized by horseradish peroxidase (DakoCytomation, Glostrup, Denmark). Fibrotic area was calculated in the picro-sirius red–stained sections by using a planimetric method with a morphometry analyzer (NIS elements D, Nikon, Japan) on 5 optical fields that were selected randomly for each sample. Extracted dog heart tissues were fixed with 2.5% glutaraldehyde, stained with uranyl acetate and lead citrate, and examined with a Hitachi H-7100 electron microscope (Hitachi High-Technologies, Tokyo, Japan).

Statistical Analysis

All data are presented as the mean ± standard error of the mean. The analyses were performed using nonparametric methods because the sample sizes were too small to allow checking of the assumptions of parametric methods. Expression of messenger RNA (mRNA) in vitro analyzed by PCR and ELISA was analyzed by Jonckheere-Terpstra test for assuring dose-dependent effect of ONO1301. Hemodynamic data obtained from conventional echocardiography, cardiac catheterization, and speckle-tracking echocardiography, as well as histopathologic findings such as percent fibrosis, cell diameter, and vascular density at the target and remote sites of control group or ONO1301SR group, were analyzed by nonparametric repeated-measures analysis. Statistical analyses were performed with the R program (R Development Core Team 2011). R: A language and environment for statistical computing. R Foundation for Statistical Computing; Vienna, Austria).

RESULTS

Effects of ONO1301 on Expression of Endogenous Cytokines In Vitro

Effects of ONO1301 on expression of HGF, VEGF, and SDF-1 in the NHDF in vitro were examined by real-time PCR and ELISA. Relative expression of mRNA for HGF, VEGF, and SDF-1 was up-regulated in the NHDF with ONO1301 added in a dose-dependent manner (Figure 1, *A-C*), which was consistent with the release of HGF, VEGF, and SDF-1 into the supernatants (Figure 1, *D-F*).

Global Recovery of the DCM Heart by Injection of ONO1301SR

Serial changes in global systolic and diastolic cardiac function were assessed under general anesthesia by conventional echocardiography at 3 time points: 0 weeks (before commencement of rapid pacing), 4 weeks after the commencement of rapid pacing (just before injection of either ONO1301SR or PLGA only), and 4 weeks after injection of either ONO1301SR or PLGA only. Cardiac performance was markedly deteriorated, including increased Dd/Ds and E/E′ and decreased EF, ESWT, and EDWT at 4 weeks, when either ONO1301MS or PLGA only was intramyocardially injected.

At 4 weeks after PLGA injection, both systolic and diastolic cardiac functions had further deteriorated.

On the other hand, EF and ESWT/ EDWT at both the target site and remote site at 4 weeks after ONO1301SR injection were significantly greater than those at 4 weeks after PLGA injection (EF, 39% ± 1.7 % vs 19% ± 2.0%; $P < .05$; Figure 2, *E*; ESWT/EDWT at target site, $1.3 \pm 3.0 \times 10^{-2}$ vs $1.1 \pm 2.0 \times 10^{-2}$; $P = .01$; Figure 2, *C*; ESWT/EDWT at remote site, 1.2 ± 0.1 vs $1.1 \pm 3.0 \times 10^{-2}$; $P = .04$; Figure 2, *D*), although the impact of the recovery was stronger in the target site. Ds was significantly smaller after ONO1301SR injection than after PLGA injection (Ds, 23 ± 2.4 vs 31 ± 1.7 mm; $P < .05$; Figure 2, *B*), whereas Dd also showed a trend to be smaller after ONO1301SR injection than after PLGA injection (Dd, 29 ± 2.3 vs 34 ± 1.4; $P < .05$; Figure 2, *A*). E/E′ after ONO1301SR injection was significantly smaller than that after PLGA injection (E/E′, 11 ± 1.2 vs 16 ± 0.5; $P < .05$; Figure 2, *F*).

Cardiac catheterization, carried out at 4 weeks after either ONO1301SR or PLGA injection, revealed that τ was significantly smaller after ONO1301SR injection than after PLGA injection (τ, 32 ± 0.9 vs 55 ± 5.8; $P < .05$). Heart rate, LV maximal systolic pressure, and maximal rate of the LV pressure change did not show any significant difference at 4 weeks after injection of either ONO1301SR or PLGA.

Regional Functional Recovery After ONO1301SR Injection

Serial changes of regional systolic cardiac function were assessed under general anesthesia by speckle-tracking echocardiography at the same 3 time points as conventional echocardiography. At 4 weeks after the commencement of rapid pacing, all strain values at both target and remote sites were decreased compared with those

ET/BS

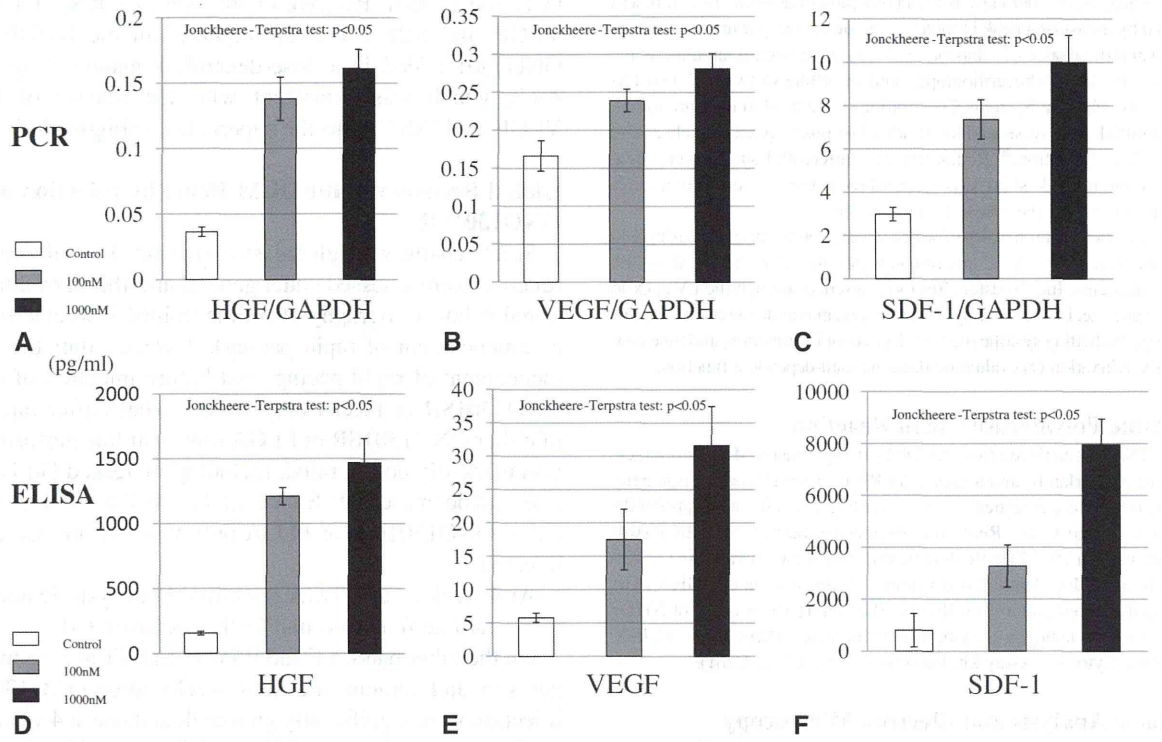

FIGURE 1. PCR and ELISA analysis in vitro showed that messenger RNA levels for HGF (A and D), VEGF (B and E), and SDF-1 (C and F) increased in a dose-dependent manner in NHDF cultured with ONO1301. *PCR*, Polymerase chain reaction; *ELISA*, enzyme-linked immunosorbent assay; *NHDF*, normal human dermal fibroblast; *HGF*, hepatocyte growth factor; *GAPDH*, glyceraldehyde-3-phosphate dehydrogenase; *SDF-1*, stromal-derived factor-1; *VEGF*, vascular endothelial growth factor. Mean ± standard error of the mean, respectively.

ET/BS

before rapid pacing. At 4 weeks after the PLGA injection, the absolute values of peak systolic radial, circumferential, transverse, and longitudinal strains at both target and remote sites further decreased compared with those before the PLGA injection. In contrast, at 4 weeks after the ONO1301SR injection, strain values of radial, transverse, and circumferential strains were greater at the target site than those after the PLGA injection (radial strain, 36% ± 4.7% vs 8.3% ± 1.4%; $P < .05$; transverse strain, 39% ± 9.3% vs 9.5% ± 2.1%; $P < .05$; circumferential strain, −11% ± 1.3% vs −3.9% ± 0.6%; $P < .05$; Figure 3, *A-C*), although longitudinal strain was not different between the hearts with and without ONO1301SR treatment (Figure 3, *D*). On the other hand, only radial strain was significantly improved at the remote site after ONO1301SR injection compared with that after PLGA injection (Figure 3, *E-H*).

Histologic Findings of Reverse LV Remodeling After ONO1301SR Injection

Gross myocardial structure, assessed by hematoxylin and eosin staining and Masson trichrome staining, showed a thicker LV wall and a smaller LV cavity 4 weeks after ONO1301SR administration (Figure 4, *H-K*) than that after PLGA injection (Figure 4, *D-G*).

Quantity of interstitial fibrosis at the target site, evaluated by picro-sirius red staining, was significantly less at 4 weeks after ONO1301SR administration compared with that after PLGA injection (percent fibrosis at the target site, 9.9% ± 0.7% vs 23% ± 0.9%; $P < .01$; Figure 4, *A*). Of note, distribution of interstitial fibrosis was significantly more restricted at the target site than that at the remote site after ONO1301SR administration (9.9% ± 0.7% vs 16% ± 1.2%), whereas PLGA injection did not produce such an uneven distribution (23% ± 0.9% at the target site vs 23% ± 0.8% at the remote site).

Mean transverse cellular diameter of cardiomyocytes (Figure 4, *B*) at the target site, measured by periodic acid-Schiff–stained sections, was also significantly smaller at 4 weeks after ONO1301SR administration compared with that after PLGA injection (12 ± 0.6 mm vs 15 ± 0.8 mm; $P < .01$). The diameter of cardiomyocytes at the target site was smaller after ONO1301SR administration compared with that at the remote site (12 ± 0.6 vs 14 ± 0.3 mm; $P < .01$), whereas such an uneven distribution in the myocyte size was not observed after PLGA injection.

Vascular density (Figure 4, *C*), assessed by counting the number of factor VIII–positive cells in the fields, was significantly greater at the target site at 4 weeks after ONO1301SR administration compared with that after